Boosting Hematopoietic Engraftment after in Utero Transplantation through Vascular Niche Manipulation

Saloomeh Mokhtari,[1] Evan J. Colletti,[2,3] Anthony Atala,[1] Esmail D. Zanjani,[2] Christopher D. Porada,[1] and Graça Almeida-Porada[1,*]

[1]Wake Forest Institute for Regenerative Medicine, Wake Forest School of Medicine, 391 Technology Way, Winston-Salem, NC 27157-1083, USA
[2]Experimental Station, University of Nevada Reno, Reno, NV 89503, USA
[3]Present address: Charles River Laboratories, Reno, NV 89511, USA
*Correspondence: galmeida@wakehealth.edu
http://dx.doi.org/10.1016/j.stemcr.2016.05.009

SUMMARY

In utero hematopoietic stem/progenitor cell transplantation (IUHSCT) has only been fully successful in the treatment of congenital immunodeficiency diseases. Using sheep as a large animal model of IUHSCT, we demonstrate that administration of $CD146^+CXCL12^+VEGFR2^+$ or $CD146^+CXCL12^+VEGFR2^-$ cells prior to, or in combination with, hematopoietic stem/progenitor cells (HSC), results in robust CXCL12 production within the fetal marrow environment, and significantly increases the levels of hematopoietic engraftment. While in the fetal recipient, donor-derived HSC were found to reside within the trabecular bone, the increased expression of VEGFR2 in the microvasculature of $CD146^+CXCL12^+VEGFR2^+$ transplanted animals enhanced levels of donor-derived hematopoietic cells in circulation. These studies provide important insights into IUHSCT biology, and demonstrate the feasibility of enhancing HSC engraftment to levels that would likely be therapeutic in many candidate diseases for IUHSCT.

INTRODUCTION

In utero hematopoietic stem cell transplantation (IUHSCT) is a clinically viable therapeutic option, which could potentially provide successful treatment for many genetic and developmental diseases affecting the immune and hematopoietic systems (MacKenzie et al., 2015). IUHSCT has safely been performed for decades in humans and is the only approach that can promise the birth of a healthy infant (Muench and Barcena, 2004; Nijagal et al., 2012). To date, its success has been limited to recipients with severe combined immunodeficiency disorders in which there is a selective advantage of donor cell engraftment/survival over host cells (Flake et al., 1996; Gotherstrom et al., 2014; Le Blanc et al., 2005; Touraine et al., 1989; Wengler et al., 1996). Because IUHSCT must be performed without myeloablation or immunosuppression, immunologic barriers and absence of stress-induced signaling have been considered as significant contributors to the limited donor HSC engraftment (Merianos et al., 2009; Nijagal et al., 2011; Peranteau et al., 2007). Other challenges observed with IUHSCT result from the unique intricacies of fetal hematopoietic stem/progenitor cell (HSC) biology and the fetal microenvironment. It has been postulated that transplanted adult cells could potentially be outcompeted by endogenous fetal HSC, since the latter are actively cycling and undergo symmetric self-renewal divisions more efficiently than adult HSC (Bowie et al., 2007). Also, the fetal microenvironment might not be appropriate to support engraftment and/or expansion of donor HSC derived from ontogenically disparate sources, as differences in membrane composition and response to cytokines exist between fetal and adult cells (Arora et al., 2014; Bowie et al., 2007; Derderian et al., 2014).

MCAM/CD146, within the adult human bone marrow (BM), is a marker of stromal progenitors/pericytes (Sacchetti et al., 2007), which produce stromal cell-derived factor 1 (SDF-1/CXCL12) and stem cell factor (SCF), and mediate HSC maintenance/retention (Corselli et al., 2013; Sugiyama et al., 2006), while VEGFR2/Flk-1 was shown to specifically define a continuous network of arterioles and sinusoidal endothelial cells within the BM, which are essential for HSC engraftment and reconstitution of hematopoiesis (Butler et al., 2010; Hooper et al., 2009; Kiel et al., 2005). Moreover, in an adult setting, CD146-expressing subendothelial cells have been shown, upon transplantation, to be able to transfer the hematopoietic microenvironment to heterotopic sites (Sacchetti et al., 2007).

Here, we investigated whether transplantation of allogeneic adult BM-derived CD146-expressing mesenchymal ($CD146^+CXCL12^+VEGFR2^-$) or endothelial ($CD146^+CXCL12^+VEGFR2^+$) cells resulted in stable long-term contribution/integration into specific fetal BM niches, and whether administration of these cells, simultaneously with, or prior to, HSC transplantation, improved levels of HSC engraftment in an in utero setting. In addition, since information about the preferential engraftment sites of adult-derived HSC within the fetal microenvironment after IUHSCT is scarce, we also investigated whether and where donor-derived HSC localized in the fetal BM, and whether they underwent cell cycling. We also evaluated, in the
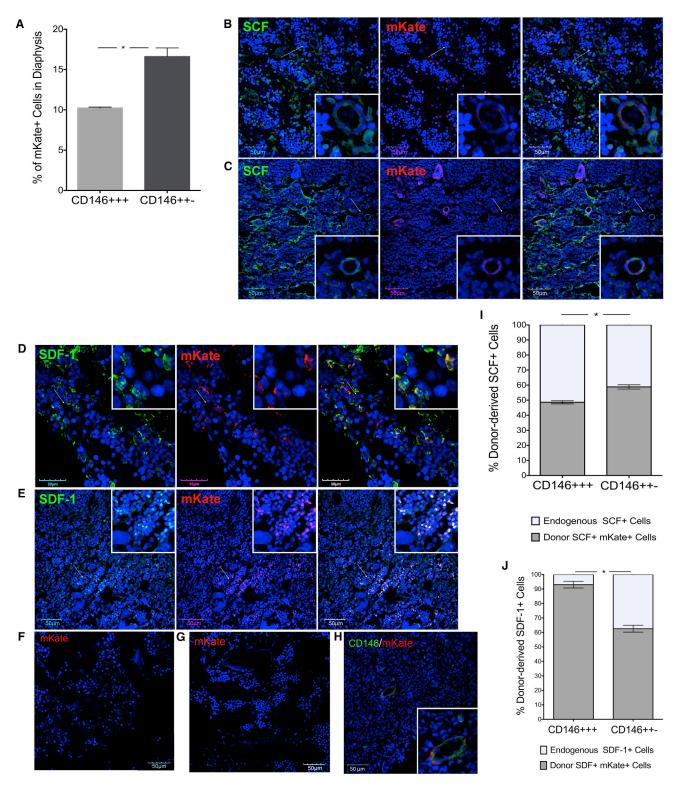
Figure 1. Engraftment Sites of CD146[++−] and CD146^{+++} Cells Transduced with an mKate-Expressing Lentivector, and Production of Endogenous and Donor-Derived SCF and CXCL12/SDF-1 in Transplanted Recipients' Diaphysis at 2–2.5 Months Post Transplant

(A) Percentage of CD146^{+++} and CD146[++−] cells engrafted in diaphysis calculated as described below. *p < 0.05.

(B–H) Representative images from the animals of in (A). (B) Production of SCF (green) by stromal perivascular and vascular cells (left panel); engrafted CD146[++−] (mKate^{+}, red) cells localized within the stromal, perivascular, and vascular niches (central panel); production

(legend continued on next page)

co-transplantation approach, whether cell-cell interactions with CD146+CXCL12+VEGFR2− or CD146+CXCL12+VEGFR2+ cells played a role in altering the patterns or levels of engraftment of subsequently transplanted HSC, and sought to identify the responsible factors. Our results show that, in a non-myeloablative fetal setting, allogeneic adult donor HSC engraft within the metaphysis, and proliferate efficiently beside endogenous hematopoietic cells, while CD146+CXCL12+VEGFR2+and CD146+CXCL12+VEGFR2− cells integrate in a different anatomic area, the bone, and/or vasculature of the diaphysis. Mechanistically, we demonstrate that CD146+CXCL12+VEGFR2+ and CD146+CXCL12+VEGFR2− cells contribute to robust CXCL12 production, and that increased expression of VEGFR2 in the microvasculature of CD146+CXCL12+VEGFR2+ transplanted animals paralleled enhanced levels of donor-derived hematopoietic cells in circulation. These studies provide additional insights into IUHSCT biology, and demonstrate the feasibility of enhancing donor HSC engraftment to levels that would likely be therapeutic in many of the diseases that are candidates for IUHSCT.

RESULTS

CD146+CXCL12+VEGFR2− and CD146+CXCL12+VEGFR2+ Cells Engraft in the Diaphysis

Fetal sheep recipients were transplanted with CD146++− or CD146+++ cells 3 days prior to, or simultaneously with, HSC and evaluated at 2–2.5 months post transplant (120–140 gestational days) as described in Experimental Procedures. Characterization of CD146+CXCL12+VEGFR2− (abbreviated as CD146++−) and CD146+CXCL12+VEGFR2+ (abbreviated as CD146+++) cells is provided in Supplemental Experimental Procedures and Figure S1. We used confocal microscopy to determine whether CD146++− or CD146+++ cells are able to durably engraft fetal recipients and to investigate the spatial distribution of the transplanted (far-red fluorescent protein [mKate]-expressing [Shcherbo et al., 2007]) CD146+++ and CD146++− cells within the trabecular (metaphysis) and cortical (diaphysis) regions.

Regardless of the transplant schedule/regimen, donor-derived CD146++− cells engrafted at significantly higher levels than CD146+++ cells (Figure 1A), and both cell populations localized primarily to the recipient diaphysis (Figures 1B–1E, central panels). Very few, if any, mKate-expressing cells were detected in the metaphysis of animals transplanted with CD146++− (Figure 1F) or CD146+++ (Figure 1G) cells.

Within the diaphysis, donor-derived CD146++− and CD146+++ cells integrated into the vascular and perivascular niches (Sacchetti et al., 2007), and continued to express CD146 (Figure 1H). In addition, engrafted CD146++− and CD146+++ cells produced SCF (Figures 1B and 1C; right/merged panel) and SDF-1/CXCL12 (Figures 1D and 1E; right/merged panel). Quantification of the relative contribution of transplanted cells to overall production of SCF and SDF-1/CXCL12 can be seen in Figures 1I and 1J, respectively. CD146+++ and CD146++− cells accounted, respectively, for 48.6% ± 1.0% and 58.8% ± 1.4% of cells positive for SCF. By contrast, as can be seen in Figures 1D and 1E (right/merged panel), SDF-1/CXCL12 expression was detected primarily in the areas where transplanted cells localized. Moreover, CD146+++ cells robustly contributed to SDF-1/CXCL12 production, such that 93% ± 2.3% of all SDF-1/CXCL12+ cells were donor derived.

Significant differences were also found with respect to the localization of the engrafted donor-derived CD146++− and CD146+++ cells (Figures 2A and 2B, respectively; right/merged panel with transmitted light display to identify bone structures). CD146++− cells were readily identified

of SCF by transplanted CD146++− cells (right panel, merged image). (C) Production of SCF (green) by stromal perivascular and vascular cells (left panel); engrafted CD146+++ (mKate+, red) cells localized within the stromal, perivascular, and vascular niches (central panel); production of SCF by transplanted CD146+++ cells (right panel, merged image). (D and E) Production of diaphyseal SDF-1/CXCL12 (green) by transplanted cells. (D) Engrafted CD146++− (mKate+, red) cells and (E) CD146+++ (mKate+, red) cells (central panels); (D) synthesis of SDF-1/CXCL12 localizes primarily to transplanted CD146++− cells and (E) robust contribution of CD146+++ cells to SDF-1/CXCL12 production (right panels, merged images). (F and G) Evaluation of metaphysis area demonstrating that neither transplanted (F) CD146++− (mKate+, red) cells, nor (G) CD146+++ (mKate+, red) cells reside within this area of the BM. (H) Within the diaphysis, donor-derived CD146+++ (mKate+, red) cells integrated into vascular structures and expressed CD146 (green).
(I) Quantification of the relative percentage of transplanted cells expressing SCF. *p < 0.05.
(J) Quantification of the relative percentage of transplanted cells expressing SDF-1/CXCL12. *p < 0.05.
Percentage of cells positive for the different specific markers was calculated after counting a total of 1,139 ± 207 DAPI+ nuclei/experiment and determining, within these, the number of cells also positive for a specific marker (n = 3 animals per group, three independent experiments). Animals were randomly selected from the pool of transplanted animals with CD146++− cells (n = 11) or CD146+++ cells (n = 7). DAPI (blue) labels all nuclei. Arrows indicate features enlarged in insets. Confocal images were acquired with an Olympus Fluoview FV1000 confocal microscope; for most of the images an Olympus UPlanFLN 40×/1.30 oil objective was used; a Plan ApoN 60×/1.42 objective was also used as noted. 60× magnification was used in (C). Confocal images were taken as z stacks with 5–10 slices per image before being projected as 2D images and saved. Detailed characterization of CD146++− and CD146+++ cells is provided in Figure S1.
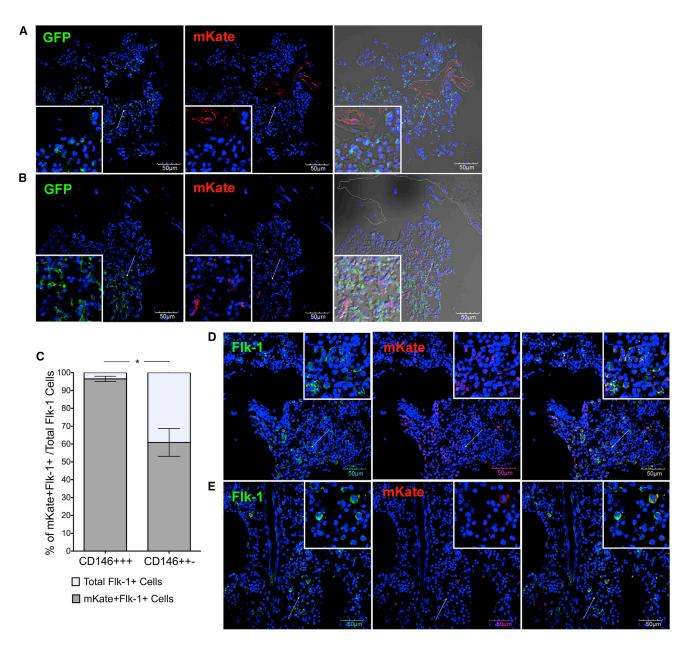
Figure 2. CD146[++−] Cells Contribute to the Vascular and Bone Niche, while CD146^{+++} Cells Engrafted Mostly in Perivascular Sites an Expressed VEGFR2/Flk-1

(A) Representative image of GFP^{+} donor-derived hematopoietic cells (green; left panel); CD146[++−] (mKate^{+}, red) cells were present at significant levels within the osteoblastic layer of the cortical bone (central panel, and right panel with transmitted light display to identify bone structures, also marked with dotted line); GFP^{+} donor-derived hematopoietic cells (green) can be seen in clusters in close proximity to donor-derived CD146[++−] bone niche cells (mKate^{+}, red; right panel).

(B) Representative image of GFP^{+} donor-derived hematopoietic cells (green; left panel); CD146^{+++} cells (mKate^{+}, red) rarely contributed to bone niches, and localized in perivascular areas (central panel). Transmitted light display (right panel) is included to identify bone structure, also marked with dotted line; GFP^{+} donor-derived hematopoietic cells (green) are often found in clusters in close proximity to CD146^{+++} vascular niche cells (mKate^{+}, red; right panel).

(C) Quantification of the relative percentage of transplanted cells expressing VEGFR2/Flk-1 Determination of percentage of cells positive for VEGFR2/Flk-1 was calculated after counting a total of 839 ± 37 DAPI[+] nuclei/experiment and determining, within these, the number of cells also positive for VEGFR2/Flk-1 (n = 3 animals per group). *$p < 0.05$.
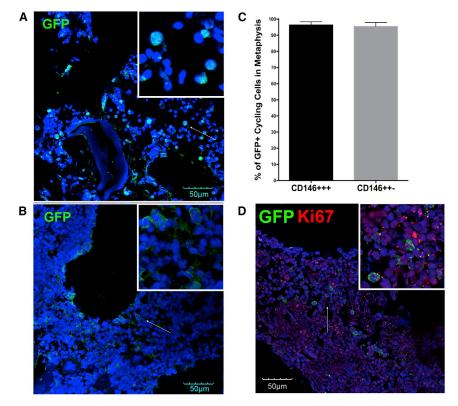
(legend continued on next page)

Figure 3. GFP⁺ Hematopoietic Cells Localize Predominantly to the Metaphysis and Are Actively Cycling

(A and B) Representative images of GFP⁺ (green) donor-derived hematopoietic cell engraftment in the trabecular bone niche of the metaphysis in animals transplanted with CD146^{++-} (A) and CD146^{+++} (B) cells.

(C) Percentage of GFP⁺ donor-derived hematopoietic cells cycling within the metaphysis, using Ki67, demonstrating that, in this area, most of the transplanted hematopoietic cells (GFP⁺) were cycling (Ki67⁺). Determination of percentage of cycling cells was accomplished by counting an average of 727 ± 80.8 DAPI⁺ nuclei per experiment, and quantifying the number of GFP⁺, Ki67⁺, and GFP⁺ Ki67⁺ double-positive cells; the percentage of cycling donor cells (GFP⁺ Ki67⁺) was then determined after normalizing to the percentage of engrafted GFP⁺ cells (n = 4 animals per group, two independent experiments).

(D) Representative image of Ki67 staining, demonstrating that donor GFP⁺ cells are cycling.

DAPI (blue) labels all nuclei. Arrows indicate features enlarged in insets. Confocal images were acquired with an Olympus FV1200 Spectral laser scanning confocal microscope and an Olympus UPlanFLN 40×/1.30 oil objective; confocal images were taken as z stacks with 5–10 slices per image before being projected as 2D images and saved. See also Figure S2.

within cortical bone structures, while CD146^{+++} rarely located to bone niches.

We next investigated the contribution of donor-derived CD146^{++-} and CD146^{+++} to VEGFR2/Flk-1 production (Figure 2C). Transplanted CD146^{+++} cells contributed to the majority of VEGFR2/Flk-1 expressed within the diaphysis (Figures 2C and 2D), and their support was significantly higher than that provided by CD146^{++-} cells (Figures 2C and 2E).

Donor-Derived Hematopoietic Cells Localize Primarily to the Trabecular Bone Niche of the Metaphysis

We next investigated which niches the donor-derived hematopoietic cells occupied, defined their relationship with transplanted stromal cell populations, and determined whether there was a preferential interaction between donor-derived (GFP⁺) HSC and donor-derived

(mKate⁺) CD146^{++-} or CD146^{+++} cells. Regardless of the cell type used for the combined transplant or the time of transplant, donor-derived GFP⁺ hematopoietic cells localized primarily to the trabecular bone niche of the metaphysis (Figures 3A and 3B) and were actively cycling, as determined by Ki67 staining, demonstrating that adult hematopoietic cells are able to effectively cycle in vivo in a fetal environment (Figures 3C and 3D).

Co-transplantation of CD146^{+++} and CD146^{++-} Cells Affects Hematopoietic Engraftment

The levels of donor-derived (GFP⁺) HSC engraftment in the BM are shown in Figure 4. Animals that received HSC 3 days after CD146^{+++} cell transplant (3^{+++}) had significantly higher levels of donor-derived hematopoietic engraftment (p < 0.05) than those receiving HSC alone (HSC) or those that received HSC concurrently with CD146^{+++} cells (0^{+++}) (Figure 4A). Colony-forming unit

(D) Robust production of VEGFR2/Flk-1 (green; left panel) by transplanted CD146^{+++} (red) cells (central panel) within diaphysis; engrafted CD146^{+++} (red) cells produce the majority of VEGFR2/Flk-1 within the perivascular niche (right panel).

(E) Production of VEGFR2/Flk-1 (green; left panel) by transplanted CD146^{++-} (red) cells (central panel) within the diaphysis; Fewer CD146^{++-} cells (mKate⁺, red) co-express VEGFR2/Flk-1 (right panel). DAPI (blue) labels all nuclei.

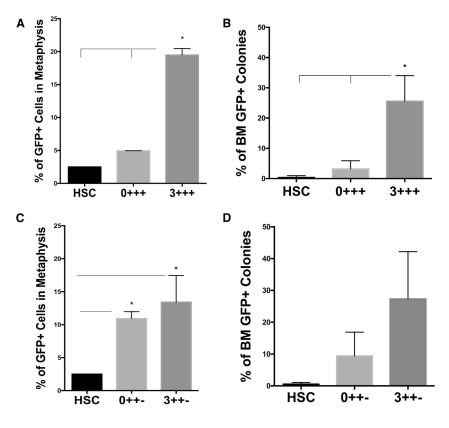Arrows indicate features enlarged in insets. Confocal images were acquired as described in Figure 1.

Figure 4. Animals Transplanted with CD146^{++-} and CD146^{+++} Cells Have Higher Levels of Donor-Derived GFP$^+$ Hematopoietic Cells

(A) Determination of levels of donor-derived GFP$^+$ HSC engraftment in the metaphysis showed that HSC3$^+$CD146^{+++} animals (n = 3 independent experiments, two animals/group) had significantly higher levels of donor-derived (GFP$^+$) HSC engraftment (*p < 0.05) than the HSC (n = 3 independent experiments, two animals/group) or the HSC0$^+$CD146^{+++} group; (n = 3 independent experiments, three animals/group).

(B) CFU assays performed using freshly collected BM from transplanted animals showed that HSC3$^+$CD146^{+++} animals contained a significantly (*p < 0.05) higher number of donor-derived (GFP$^+$) CFU than the other transplant groups (n = 3 animals per group, except for HSC3$^+$CD146^{+++} and HSC, n = 2 animals per group; each with n = 3 technical replicates).

(C) HSC3$^+$CD146^{++-} and HSC0$^+$CD146^{++-} animals had significantly higher HSC engraftment (*p < 0.05) than the HSC group (n = 3 animals/group; three independent experiments).

(D) CFU assays performed using freshly collected BM from transplanted animals showed that HSC3$^+$CD146^{++-} animals contained a higher number of donor-derived (GFP$^+$) CFU than the other transplant groups, but statistical significance was not achieved (n = 3 animals/group; each with n = 3 technical replicates).

(CFU) assays, performed using freshly collected BM, showed that 3^{+++} animals contained a significantly (p < 0.05) higher number of donor-derived (GFP$^+$) CFU than the other transplant groups, attesting to the higher clonogenic potential of the engrafted cells in this group (Figure 4B). Of note, concurrent transplantation of HSC and CD146^{+++} cells (0^{+++}) did not significantly increase the clonogenic potential of the engrafted cells beyond that seen with HSC alone (Figure 4B).

In the metaphysis of animals that received HSC 3 days after CD146^{++-} cell transplant (3^{++-}) and HSC simultaneously with CD146^{++-} cells (0^{++-}), the percentage of donor-derived HSC engraftment was significantly higher (p < 0.05) than in the group transplanted with HSC alone (HSC) (Figure 4C). However, no statistical significance was found between the percentage of donor-derived hematopoietic engraftment and clonogenic potential of engrafted cells in animals that received 3^{++-} and 0^{++-} (Figure 4D).

Analysis of the diaphysis also demonstrated that, in all of the recipients (Figures 5A and 5B), smaller numbers of donor-derived GFP$^+$ hematopoietic cells were present in this region, but localized in clusters in close proximity to

mKate$^+$ (donor) niche cells (Figures 5A and 5B; right/merged panels) in areas close to the vasculature.

In the diaphysis, quantitative analysis of mKate$^+$CD146$^+$ cells in forming vasculature demonstrated that, in this area, there was a direct correlation between the levels of donor-derived mKate$^+$CD146$^+$ cells engrafted within the vasculature and the numbers of donor-derived GFP$^+$ hematopoietic cells present in the perivascular areas (defined as being within a distance of five nuclei from a vessel) (Figure 5C).

CD146^{+++} Cells Have a Significant Effect on the Levels of Donor-Derived Hematopoiesis in Peripheral Blood

We next investigated the impact of transplanting CD146^{+++} or CD146^{++-} cells simultaneously with HSC (0^{+++} and 0^{++-}, respectively), or 3 days prior to HSC (3^{+++} and 3^{++-}, respectively), on the repopulation of peripheral blood (PB) with donor-derived hematopoiesis. At 2–2.5 months post transplant, the levels of circulating donor-derived hematopoietic cells were compared between animals that received HSC, 0^{+++}, 3^{+++}, 0^{++-}, and 3^{++-}. Flow cytometric evaluation of GFP$^+$ cells in PB demonstrated that 3^{+++} recipients had significantly higher circulating
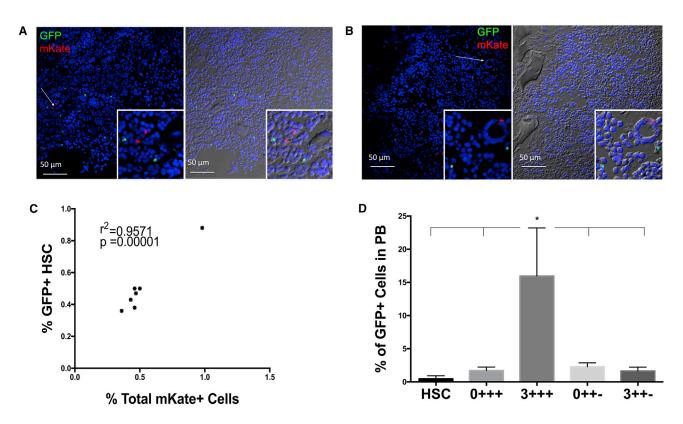
Figure 5. Smaller Numbers of Donor-Derived GFP⁺ Hematopoietic Cells Were Present in the Diaphysis, and a Correlation Existed between the Levels of Donor-Derived CD146⁺ Cells Engrafted within the Vasculature and the Numbers of Donor-Derived GFP⁺ Hematopoietic Cells Present in the Perivascular Areas

(A and B) GFP⁺ hematopoietic cells in the diaphysis of animals transplanted with either (A) CD146++− or (B) CD146+++ cells. GFP⁺ cells were found in close proximity to CD146++− or CD146+++ (mKate⁺, red) cells. DAPI (blue) labels all nuclei. Arrows indicate features enlarged in insets. Confocal images were acquired as described in Figure 1.

(C) Correlation between the numbers of donor-derived CD146⁺ cells (red) engrafted within the vasculature and the numbers of donor-derived GFP⁺ hematopoietic cells present in the perivascular areas (defined as being within a distance of five nuclei from vessel) (n = 7 animals).

(D) Percentages of circulating donor hematopoietic cells in animals transplanted with different cell populations determined by flow cytometric analysis (*$p < 0.05$). n = 3 animals per group and two independent experiments, except for HSC3⁺CD146+++ and HSC groups (n = 2 animals per group with two independent experiments).

levels of donor cells ($p < 0.05$) than those receiving HSC alone, 0+++, 3++−, or 0++− (Figure 5D).

Donor-Derived HSC Are Not Detected within the Fetal Liver of Transplanted Animals

We next performed studies to confirm that donor-derived hematopoiesis was mainly localized to the BM, and that the higher levels of donor hematopoietic cells in circulation seen with some of the transplanted groups were not due to establishment of donor-derived hematopoiesis within the liver of the fetal recipients. No donor (GFP⁺) hematopoietic cells were detected in the liver of any of the transplanted animals, regardless of the transplantation scheme (Figure 6A, left panel), despite the presence of host/recipient CD45⁺ cells within this tissue (Figure 6A,

right panel). Of note is that, after in utero transplantation, both donor-derived mKate⁺ stromal cell populations were detected at significant levels within the hepatic parenchyma (Figures 6B and 6C [central panels], and Figure 6D).

Elevation of SDF-1 levels in PB can mobilize HSC to the circulation, with a concomitant decrease of HSC within the BM (Hattori et al., 2003). Because mKate⁺ CD146+++ and CD146++− stromal cells in the BM produced SDF-1, we next investigated whether donor-derived stromal cells contributed to SDF-1 production following engraftment within the fetal liver. As previously described (Coulomb-L'Hermin et al., 1999; Kollet et al., 2003), SDF-1⁺ cells were present within the hepatic parenchyma, but, in contrast to what we observed within the BM, very few of the mKate⁺ CD146+++ or CD146++− donor cells that
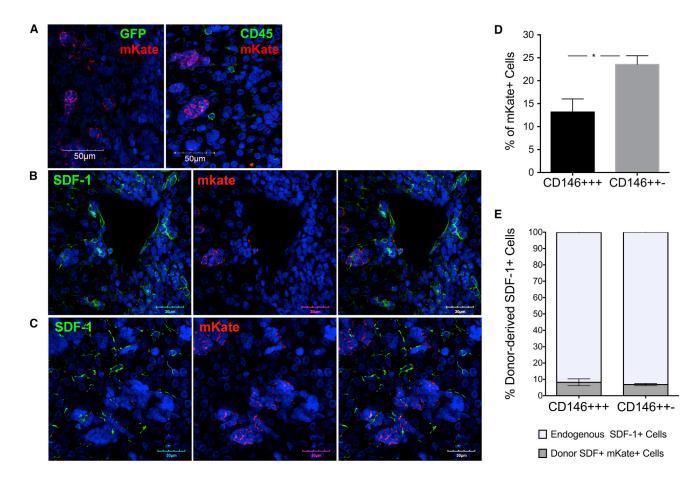
Figure 6. Donor-Derived mKate⁺ Cells, but Not GFP⁺ Donor-Derived Hematopoietic Cells, Are Detected within the Fetal Liver of Transplanted Animals

(A) Regardless of the transplantation scheme, donor-derived (GFP⁺) hematopoietic cells were not detected in the liver of any of the transplanted animals, even after staining with an antibody against GFP (left panel), and despite the ability to detect host/recipient CD45⁺ cells within this tissue (right panel) using an antibody against CD45; mKate⁺ (red) CD146⁺⁺⁻ and CD146⁺⁺⁺ cells were readily detected.

(B and C) CXCL12/SDF-1⁺ cells were present within the hepatic parenchyma of transplanted animals (left panels); very few of the donor-derived (mKate⁺, red) CD146⁺⁺⁻ (B) and CD146⁺⁺⁺ (C) cells expressed this chemokine.

(D) Percentage of CD146⁺⁺⁺ and CD146⁺⁺⁻ cells engrafted in liver calculated as described below. *p < 0.05.

(E) Quantification of the relative percentage of transplanted cells expressing SDF-1. Determination of percentage of positive cells for the different markers was calculated after counting a total of 222 ± 18 DAPI⁺ nuclei/experiment and determining, within these, the number of cells also positive for the respective markers (n = 3 per group).

DAPI (blue) labels all nuclei. Confocal images were acquired as described in Figure 3.

engrafted the liver continued to express this chemokine (Figures 6B and 6C). A graphical depiction of the relative contribution of donor-derived CD146⁺⁺⁺ and CD146⁺⁺⁻ cells to overall SDF-1 production within the recipient fetal liver is shown in Figure 6E.

DISCUSSION

Similarly to unconditioned adult recipients, transplantation of allogeneic HSC into non-ablated fetal hosts faces serious challenges. Immunologic barriers posed by the mother's immune system (Merianos et al., 2009; Nijagal et al., 2011) and by the emerging innate and adaptive immunity of the host (Bhattacharya et al., 2006; De Kleer et al., 2014; Peranteau et al., 2007; Rechavi et al., 2015; Renoux et al., 2015; Szepfalusi et al., 2000; Xu et al., 2004) can lead to graft rejection, or at least significant graft loss, before donor-specific tolerance is achieved (Peranteau et al., 2015). For example, in non-irradiated adult animals, only continuous infusion (Wright et al., 2001) or transplantation of extraordinarily high doses of BM HSC (Rao et al., 1997) have resulted in hematopoietic chimerism; such approaches would be challenging to implement in a fetal setting.

Robust long-term engraftment of adult-derived cells in a fetal setting also depends upon the ability of adult cells to effectively compete with endogenous cells for the appropriate niches (Bhattacharya et al., 2006; Calvi et al., 2003; Ding et al., 2012; Greenbaum et al., 2013; Kunisaki et al., 2013) and the existence of fully functional microenvironments (Jeanblanc et al., 2014) that can support/promote adult hematopoiesis.

The fetal sheep model (Flake et al., 1986) has proved to be instrumental in developing strategies for IUHSCT, since it is outbred and therefore genetically diverse, and parallels human immune and hematopoietic development; moreover, data collected in this model were used by Flake et al. (1996) to design the transplantation approach to achieve the first clinical cure with IUHSCT. Nevertheless, like any other animal model, sheep cannot exactly reproduce all the features of human pregnancy. For instance, probably due to the type of placentation, ewes do not modulate maternal immunity toward a more tolerogenic phenotype, and therefore the role of maternal immunity in fetal transplant rejection cannot be addressed in this model (Entrican et al., 2015).

Nevertheless, using this model, we demonstrated the possibility of increasing hematopoietic engraftment after IUHSCT by the administration of stromal elements (Almeida-Porada et al., 1999, 2000). However, we did not characterize which populations within the adult stromal cells were responsible for the effect, nor did we address the interaction between transplanted HSC and stromal cells or the long-term fate and localization of the transplanted cell populations, leaving unanswered the questions of whether and where within the BM these cells lodged.

In these studies, we show that CD146^{++-} or CD146^{+++} cells are responsible for the significant increase in the levels of donor-derived hematopoietic engraftment, and that CD146^{++-} and CD146^{+++} cells engrafted long-term, localized almost exclusively within the diaphysis of the fetal BM, and integrated within the bone and perivascular niches. By contrast, transplanted CD146^{++-} and CD146^{+++} cells did not reside within the metaphysis of fetal recipients. Unexpectedly, the vast majority of the transplanted HSC, independent of the transplantation schedule/approach, were found within the metaphysis, where they were actively cycling, demonstrating that adult cells can efficiently divide in the fetal microenvironment. Since our analysis was performed at over 2 months after IUHSCT, the results obtained reflect an examination of the localization of the transplanted HSC in the "steady state," after durable engraftment took place.

We also show that a direct correlation exists between the levels of donor-derived CD146^{++-} or CD146^{+++} cells within perivascular regions of the diaphysis and the levels of donor hematopoietic engraftment seen in the vicinity (within five cell nuclei) of vasculature containing donor-derived niche cells. This finding could suggest that providing an adult-derived perivascular niche enables more donor-derived HSC to migrate to or engraft within the BM. During fetal development, long bones are the primary site for BM hematopoiesis (Proytcheva, 2013) and, given that blood flow through the long bones proceeds mostly from the diaphysis to the metaphysis, the engraftment of CD146^{++-} CD146^{+++} cells within the diaphysis and their production of hematopoiesis-supporting chemokines may serve to attract transplanted HSC to the marrow cavity, from whence they are then drawn to the metaphysis by the active bone remodeling at this stage of development and by the high hyaluronic acid synthase levels present in that region (Figure S2, top panel) when compared with the diaphysis of fetal sheep (Figure S2, lower panel).

These data are in agreement with prior studies demonstrating that hyaluronan levels play a critical role in determining the site of HSC lodgment/engraftment following transplantation (Avigdor et al., 2004; Ellis et al., 2007, 2009, 2011; Nilsson et al., 2003), and that HSC exhibit preferential engraftment within sites of active bone remodeling (Chan et al., 2009).

In the adult, SDF-1/CXCL12 plays a critical role in BM repopulation by circulating CD34$^+$ progenitors (Peled et al., 1999a, 1999b), and during development, SDF-1 induces the migration of primitive HSC from the fetal liver to the BM (Ma et al., 1998) and promotes HSC colonization (Ara et al., 2003). Likewise, membrane-bound SCF is important for HSC maintenance (Barker, 1997) and myeloid development after transplantation (Takagi et al., 2012). Both CD146^{++-} and CD146^{+++} cells expressed, in vitro and after in vivo engraftment, SDF-1 and SCF. However, our analyses also showed that SCF is ubiquitously present within the fetal microenvironment, suggesting that SCF provided by the transplanted cells is not likely to be responsible for the observed enhancement in engraftment. By contrast, BM immunohistochemistry of transplanted animals showed robust SDF-1/CXCL12 production by transplanted CD146^{+++} cells. The production of SDF-1/CXCL12 at the site of HSC entrance/exit provides a potential explanation for the increased HSC engraftment seen in the co-transplanted animals over those receiving HSC alone.

CD146^{+++} and CD146^{++-} cells seem to affect HSC engraftment through some additional cell-specific mechanism, since CD146^{+++} cells only produced a statistically significant increase in BM donor hematopoietic engraftment if they were administered 3 days prior to the HSC. In contrast, CD146^{++-} cells enhanced BM hematopoietic engraftment whether they were administered 3 days prior to the HSC graft or concomitantly with it. The ability of CD146^{++-}, but not CD146^{+++}, cells to enhance hematopoietic engraftment when transplanted simultaneously with the HSC, suggests that the effect of CD146^{++-} cells could be mediated, at least

in part, by their ability to alter the innate and adaptive immune responses (Domev et al., 2014; English et al., 2010; Le Blanc and Davies, 2015; Le Blanc et al., 2007), perhaps protecting the transplanted HSC from the rudimentary immune elements present within the fetus at this stage of gestation (Skopal-Chase et al., 2009).

Our data also show that HSC3⁺CD146⁺⁺⁺ animals exhibit significantly higher levels of overall hematopoietic cell engraftment than any other group. In vitro, and after engraftment, CD146⁺⁺⁺ cells strongly expressed VEGFR2 while CD146⁺⁺⁻ cells did not, suggesting that, even in the absence of injury to the vascular niche (Hooper et al., 2009), VEGFR2 seems to play a role in increasing hematopoietic engraftment in the fetal recipient. This could be due to VEGFR2's ability to promote survival of hematopoietic progenitors through the activation of anti-apoptotic pathways (Larrivee et al., 2003) and/or stimulating the formation of hematopoietic-supporting hemospheres (Wang et al., 2013).

It is also of note that the data presented here corroborate reports demonstrating that mesenchymal stromal cells transplanted in utero contribute to the forming bone, and could therefore be of clinical benefit for patients with osteogenesis imperfecta (Gotherstrom et al., 2014). More importantly, we demonstrate that a substantial fraction of transplanted stromal cells were found in the liver and never reached the BM, underscoring the need for defining strategies to increase bone engraftment of mesenchymal cells after in utero transplantation (Jones et al., 2012; Millard et al., 2015).

Overall, these studies demonstrate that in a fetal setting, transplanted HSC locate primarily in the metaphysis, and that both CD146⁺⁺⁻ and CD146⁺⁺⁺ stromal cells contribute, long-term, to the different BM niches and influence hematopoiesis through CXCL12, crucial for successful HSC engraftment in a fetal setting. Moreover, we show the feasibility of using a co-transplantation strategy that significantly (>10-fold) enhances donor HSC engraftment following IUHSCT. Because stromal cells have been transplanted safely in fetal recipients, confirmation of these results in another preclinical model would allow this straightforward and clinically viable approach to be used in a clinical setting to achieve levels of hematopoietic cell engraftment that would likely be therapeutic in many of the diseases that are candidates for treatment by IUHSCT.

EXPERIMENTAL PROCEDURES

Isolation and Expansion of Sheep BM-Derived Stromal Cells and Hematopoietic Stem/Progenitor Cells

Sheep BM mononuclear cells (BMMNC) were isolated from the BM of adult (2–3 years old) ewes by Ficoll density gradient (Histopaque 1077; Sigma) centrifugation, according to approved Institutional

Animal Care and Use Committee (IACUC) guidelines. Two different stromal cell populations were isolated, one with mesenchymal progenitor cell activity (CD146⁺⁺⁻) and another with sinusoidal endothelial progenitor characteristics (CD146⁺⁺⁺). Details about isolation and culture of these cells are provided in Supplemental Experimental Procedures. Sheep CD34⁺ HSC were isolated from BMMNC by positive selection using anti-sheep CD34 (Genovac) and the MidiMACS system (Miltenyi Biotec) as previously described (Porada et al., 2008).

Characterization of CD146⁺⁺⁻ or CD146⁺⁺⁺ Cells by Immunocytochemistry and Tube-Formation Assay

To better characterize cell phenotype and functionality, we performed immunocytochemistry and tube-formation assays as detailed in Supplemental Experimental Procedures. For determination of whether CD146⁺⁺⁻ cells fulfilled the criteria of mesenchymal progenitors, these cells were induced to differentiate into adipocytes and osteocytes as previously described (Soland et al., 2012) and as detailed in Supplemental Experimental Procedures.

Lentiviral Vector Transduction

To facilitate tracking post-transplantation, we transduced CD146⁺⁺⁺ or CD146⁺⁺⁻ cells with the LVmKate-2 lentivector, and CD34⁺ HSCs with the Lv105-eGFP lentivector (both from Capital Biosciences), as detailed in Supplemental Experimental Procedures. CFU assays were performed to confirm preservation of hematopoietic engraftment capability (Wiley and Yeager, 1991).

In Utero Transplantation and Tissue Collection

A total of 33 animals were used in these studies. Fetal sheep were injected intraperitoneally at 60–65 gestational days, which corresponds to ~16–17 weeks of gestation in humans, by ultrasound-guided transabdominal percutaneous injection as described by Chamberlain et al. (2007), and in accordance with IACUC guidelines, with different subsets of cells derived from the same donor: (1) CD146⁺⁺⁻ and HSC simultaneously (n = 14); (2) CD146⁺⁺⁻ followed by HSC 3 days later (n = 4); (3) CD146⁺⁺⁺ and HSC simultaneously (n = 5); (4) CD146⁺⁺⁺, followed by HSC 3 days later (n = 4); or (5) HSC alone (n = 4). CD146⁺⁺⁻ cells, CD146⁺⁺⁺ cells, and HSC were administered at a dose of 2.5×10^6/kg, 7.1×10^6/kg, and 2.1×10^6/kg, respectively. Non-transplanted animals (n = 2) were used as controls.

Colony-Forming Cell Assays

BM aspirates were collected from the iliac crest at the time of euthanasia. Methylcellulose colony assays were performed by plating 10,000 BMMNC in MethoCult GF H4330 (StemCell Technologies) supplemented with PHA-stimulated sheep leukocyte-conditioned medium (PHA-LCM) (5% v/v), as previously described (Porada et al., 2008). The percentage of GFP⁺ colonies was calculated by dividing the number of GFP⁺ colonies by the total number of GFP⁺ and GFP⁻ colonies.

Flow Cytometric Analysis

Flow cytometric analysis was performed to assess levels of donor hematopoietic cell engraftment. For evaluation of the percentage

of donor-derived GFP$^+$ CD45$^+$ cells within the PB and BM, cells were stained with RPE-conjugated anti-ovine CD45 (Serotec; MCA2220PE) and fluorescein isothiocyanate (FITC)-conjugated ANTI-GFP antibody (Abcam; ab66180), and analyzed on a FACSCalibur (Becton Dickinson Immunocytometry Systems). Negative controls included: mouse immunoglobulin 1 (IgG1) RPE isotype negative control (Serotec; MCA928RPE) and rabbit IgG FITC isotype control (Abcam; ab37406).

Immunohistochemistry

Long bones were collected, processed, and stained with antibodies to the lentivector-encoded reporter genes, cell-specific markers, and Ki67, as detailed in Supplemental Experimental Procedures, to examine the localization of the transplanted cells within the fetal sheep BM, levels of HSC engraftment, and proliferative status.

Statistical Analysis

All data are presented as mean ± SEM. We used GraphPad Prism 6 (GraphPad Software) for statistical analysis, and ordinary one-way ANOVA followed by a Holm-Sidak multiple comparisons test with a singled pooled variance. Spearman's correlation tests were applied to evaluate correlations. For all analyses, p $\leq$ 0.05 was considered to be statistically significant.

SUPPLEMENTAL INFORMATION

Supplemental Information includes Supplemental Experimental Procedures and two figures and can be found with this article online at http://dx.doi.org/10.1016/j.stemcr.2016.05.009.

REFERENCES

Almeida-Porada, G., Flake, A.W., Glimp, H.A., and Zanjani, E.D. (1999). Cotransplantation of stroma results in enhancement of engraftment and early expression of donor hematopoietic stem cells in utero. Exp. Hematol. *27*, 1569–1575.

Almeida-Porada, G., Porada, C.D., Tran, N., and Zanjani, E.D. (2000). Cotransplantation of human stromal cell progenitors into preimmune fetal sheep results in early appearance of human donor cells in circulation and boosts cell levels in bone marrow at later time points after transplantation. Blood *95*, 3620–3627.

Ara, T., Tokoyoda, K., Sugiyama, T., Egawa, T., Kawabata, K., and Nagasawa, T. (2003). Long-term hematopoietic stem cells require stromal cell-derived factor-1 for colonizing bone marrow during ontogeny. Immunity *19*, 257–267.

Arora, N., Wenzel, P.L., McKinney-Freeman, S.L., Ross, S.J., Kim, P.G., Chou, S.S., Yoshimoto, M., Yoder, M.C., and Daley, G.Q. (2014). Effect of developmental stage of HSC and recipient on transplant outcomes. Dev. Cell *29*, 621–628.

Avigdor, A., Goichberg, P., Shivtiel, S., Dar, A., Peled, A., Samira, S., Kollet, O., Hershkoviz, R., Alon, R., Hardan, I., et al. (2004). CD44 and hyaluronic acid cooperate with SDF-1 in the trafficking of human CD34$^+$ stem/progenitor cells to bone marrow. Blood *103*, 2981–2989.

Barker, J.E. (1997). Early transplantation to a normal microenvironment prevents the development of steel hematopoietic stem cell defects. Exp. Hematol. *25*, 542–547.

Bhattacharya, D., Rossi, D.J., Bryder, D., and Weissman, I.L. (2006). Purified hematopoietic stem cell engraftment of rare niches corrects severe lymphoid deficiencies without host conditioning. J. Exp. Med. *203*, 73–85.

Bowie, M.B., Kent, D.G., Copley, M.R., and Eaves, C.J. (2007). Steel factor responsiveness regulates the high self-renewal phenotype of fetal hematopoietic stem cells. Blood *109*, 5043–5048.

Butler, J.M., Nolan, D.J., Vertes, E.L., Varnum-Finney, B., Kobayashi, H., Hooper, A.T., Seandel, M., Shido, K., White, I.A., Kobayashi, M., et al. (2010). Endothelial cells are essential for the self-renewal and repopulation of notch-dependent hematopoietic stem cells. Cell Stem Cell *6*, 251–264.

Calvi, L.M., Adams, G.B., Weibrecht, K.W., Weber, J.M., Olson, D.P., Knight, M.C., Martin, R.P., Schipani, E., Divieti, P., Bringhurst, F.R., et al. (2003). Osteoblastic cells regulate the haematopoietic stem cell niche. Nature *425*, 841–846.

Chamberlain, J., Yamagami, T., Colletti, E., Theise, N.D., Desai, J., Frias, A., Pixley, J., Zanjani, E.D., Porada, C.D., and Almeida-Porada, G. (2007). Efficient generation of human hepatocytes by the intrahepatic delivery of clonal human mesenchymal stem cells in fetal sheep. Hepatology *46*, 1935–1945.

Chan, C.K., Chen, C.C., Luppen, C.A., Kim, J.B., DeBoer, A.T., Wei, K., Helms, J.A., Kuo, C.J., Kraft, D.L., and Weissman, I.L. (2009). Endochondral ossification is required for haematopoietic stem-cell niche formation. Nature *457*, 490–494.

Corselli, M., Chin, C.J., Parekh, C., Sahaghian, A., Wang, W., Ge, S., Evseenko, D., Wang, X., Montelatici, E., Lazzari, L., et al. (2013). Perivascular support of human hematopoietic stem/progenitor cells. Blood *121*, 2891–2901.

Coulomb-L'Hermin, A., Amara, A., Schiff, C., Durand-Gasselin, I., Foussat, A., Delaunay, T., Chaouat, G., Capron, F., Ledee, N., Galanaud, P., et al. (1999). Stromal cell-derived factor 1 (SDF-1) and antenatal human B cell lymphopoiesis: expression of SDF-1 by

mesothelial cells and biliary ductal plate epithelial cells. Proc. Natl. Acad. Sci. USA *96*, 8585–8590.

De Kleer, I., Willems, F., Lambrecht, B., and Goriely, S. (2014). Ontogeny of myeloid cells. Front. Immunol. *5*, 423.

Derderian, S.C., Togarrati, P.P., King, C., Moradi, P.W., Reynaud, D., Czechowicz, A., Weissman, I.L., and MacKenzie, T.C. (2014). In utero depletion of fetal hematopoietic stem cells improves engraftment after neonatal transplantation in mice. Blood *124*, 973–980.

Ding, L., Saunders, T.L., Enikolopov, G., and Morrison, S.J. (2012). Endothelial and perivascular cells maintain haematopoietic stem cells. Nature *481*, 457–462.

Domev, H., Milkov, I., Itskovitz-Eldor, J., and Dar, A. (2014). Immunoevasive pericytes from human pluripotent stem cells preferentially modulate induction of allogeneic regulatory T cells. Stem Cells Transl. Med. *3*, 1169–1181.

Ellis, S., Williams, B., Asquith, S., Rutherford, K., Haylock, D., Bertoncello, I., Nilsson, S., and Camenisch, T. (2007). Hyaluronan, a key component in the hemopoietic stem cell niche. Microsc. Microanal. *13*, 356–357.

Ellis, S.L., Williams, B., Asquith, S., Bertoncello, I., and Nilsson, S.K. (2009). An innovative triple immunogold labeling method to investigate the hemopoietic stem cell niche in situ. Microsc. Microanal. *15*, 403–414.

Ellis, S.L., Grassinger, J., Jones, A., Borg, J., Camenisch, T., Haylock, D., Bertoncello, I., and Nilsson, S.K. (2011). The relationship between bone, hemopoietic stem cells, and vasculature. Blood *118*, 1516–1524.

English, K., French, A., and Wood, K.J. (2010). Mesenchymal stromal cells: facilitators of successful transplantation? Cell Stem Cell *7*, 431–442.

Entrican, G., Wattegedera, S.R., and Griffiths, D.J. (2015). Exploiting ovine immunology to improve the relevance of biomedical models. Mol. Immunol. *66*, 68–77.

Flake, A.W., Harrison, M.R., Adzick, N.S., and Zanjani, E.D. (1986). Transplantation of fetal hematopoietic stem cells in utero: the creation of hematopoietic chimeras. Science *233*, 776–778.

Flake, A.W., Roncarolo, M.G., Puck, J.M., Almeida-Porada, G., Evans, M.I., Johnson, M.P., Abella, E.M., Harrison, D.D., and Zanjani, E.D. (1996). Treatment of X-linked severe combined immunodeficiency by in utero transplantation of paternal bone marrow. N. Engl. J. Med. *335*, 1806–1810.

Gotherstrom, C., Westgren, M., Shaw, S.W., Astrom, E., Biswas, A., Byers, P.H., Mattar, C.N., Graham, G.E., Taslimi, J., Ewald, U., et al. (2014). Pre- and postnatal transplantation of fetal mesenchymal stem cells in osteogenesis imperfecta: a two-center experience. Stem Cells Transl. Med. *3*, 255–264.

Greenbaum, A., Hsu, Y.M., Day, R.B., Schuettpelz, L.G., Christopher, M.J., Borgerding, J.N., Nagasawa, T., and Link, D.C. (2013). CXCL12 in early mesenchymal progenitors is required for haematopoietic stem-cell maintenance. Nature *495*, 227–230.

Hattori, K., Heissig, B., and Rafii, S. (2003). The regulation of hematopoietic stem cell and progenitor mobilization by chemokine SDF-1. Leuk. Lymphoma *44*, 575–582.

Hooper, A.T., Butler, J.M., Nolan, D.J., Kranz, A., Iida, K., Kobayashi, M., Kopp, H.-G., Shido, K., Petit, I., Yanger, K., et al. (2009).

Engraftment and reconstitution of hematopoiesis is dependent on VEGFR2-mediated regeneration of sinusoidal endothelial cells. Cell Stem Cell *4*, 263–274.

Jeanblanc, C., Goodrich, A.D., Colletti, E., Mokhtari, S., Porada, C.D., Zanjani, E.D., and Almeida-Porada, G. (2014). Temporal definition of haematopoietic stem cell niches in a large animal model of in utero stem cell transplantation. Br. J. Haematol. *166*, 268–278.

Jones, G.N., Moschidou, D., Lay, K., Abdulrazzak, H., Vanleene, M., Shefelbine, S.J., Polak, J., de Coppi, P., Fisk, N.M., and Guillot, P.V. (2012). Upregulating CXCR4 in human fetal mesenchymal stem cells enhances engraftment and bone mechanics in a mouse model of osteogenesis imperfecta. Stem Cells Transl. Med. *1*, 70–78.

Kiel, M.J., Yilmaz, O.H., Iwashita, T., Terhorst, C., and Morrison, S.J. (2005). SLAM family receptors distinguish hematopoietic stem and progenitor cells and reveal endothelial niches for stem cells. Cell *121*, 1109–1121.

Kollet, O., Shivtiel, S., Chen, Y.Q., Suriawinata, J., Thung, S.N., Dabeva, M.D., Kahn, J., Spiegel, A., Dar, A., Samira, S., et al. (2003). HGF, SDF-1, and MMP-9 are involved in stress-induced human CD34+ stem cell recruitment to the liver. J. Clin. Invest. *112*, 160–169.

Kunisaki, Y., Bruns, I., Scheiermann, C., Ahmed, J., Pinho, S., Zhang, D., Mizoguchi, T., Wei, Q., Lucas, D., Ito, K., et al. (2013). Arteriolar niches maintain haematopoietic stem cell quiescence. Nature *502*, 637–643.

Larrivee, B., Lane, D.R., Pollet, I., Olive, P.L., Humphries, R.K., and Karsan, A. (2003). Vascular endothelial growth factor receptor-2 induces survival of hematopoietic progenitor cells. J. Biol. Chem. *278*, 22006–22013.

Le Blanc, K., and Davies, L.C. (2015). Mesenchymal stromal cells and the innate immune response. Immunol. Lett. *168*, 140–146.

Le Blanc, K., Gotherstrom, C., Ringden, O., Hassan, M., McMahon, R., Horwitz, E., Anneren, G., Axelsson, O., Nunn, J., Ewald, U., et al. (2005). Fetal mesenchymal stem-cell engraftment in bone after in utero transplantation in a patient with severe osteogenesis imperfecta. Transplantation *79*, 1607–1614.

Le Blanc, K., Samuelsson, H., Gustafsson, B., Remberger, M., Sundberg, B., Arvidson, J., Ljungman, P., Lonnies, H., Nava, S., and Ringden, O. (2007). Transplantation of mesenchymal stem cells to enhance engraftment of hematopoietic stem cells. Leukemia *21*, 1733–1738.

Ma, Q., Jones, D., Borghesani, P.R., Segal, R.A., Nagasawa, T., Kishimoto, T., Bronson, R.T., and Springer, T.A. (1998). Impaired B-lymphopoiesis, myelopoiesis, and derailed cerebellar neuron migration in CXCR4- and SDF-1-deficient mice. Proc. Natl. Acad. Sci. USA *95*, 9448–9453.

MacKenzie, T.C., David, A.L., Flake, A.W., and Almeida-Porada, G. (2015). Consensus statement from the first international conference for in utero stem cell transplantation and gene therapy. Front. Pharmacol. *6*, 15.

Merianos, D.J., Tiblad, E., Santore, M.T., Todorow, C.A., Laje, P., Endo, M., Zoltick, P.W., and Flake, A.W. (2009). Maternal alloantibodies induce a postnatal immune response that limits engraftment following in utero hematopoietic cell transplantation in mice. J. Clin. Invest. *119*, 2590–2600.

Millard, S.M., Pettit, A.R., Ellis, R., Chan, J.K.Y., Raggatt, L.J., Khosrotehrani, K., and Fisk, N.M. (2015). Intrauterine bone marrow transplantation in osteogenesis imperfecta mice yields donor osteoclasts and osteomacs but not osteoblasts. Stem Cell Rep. 5, 682–689.

Muench, M.O., and Barcena, A. (2004). Stem cell transplantation in the fetus. Cancer Control 11, 105–118.

Nijagal, A., Wegorzewska, M., Jarvis, E., Le, T., Tang, Q., and MacKenzie, T.C. (2011). Maternal T cells limit engraftment after in utero hematopoietic cell transplantation in mice. J. Clin. Invest. 121, 582–592.

Nijagal, A., Flake, A.W., and MacKenzie, T.C. (2012). In utero hematopoietic cell transplantation for the treatment of congenital anomalies. Clin. Perinatol. 39, 301–310.

Nilsson, S.K., Haylock, D.N., Johnston, H.M., Occhiodoro, T., Brown, T.J., and Simmons, P.J. (2003). Hyaluronan is synthesized by primitive hemopoietic cells, participates in their lodgment at the endosteum following transplantation, and is involved in the regulation of their proliferation and differentiation in vitro. Blood 101, 856–862.

Peled, A., Grabovsky, V., Habler, L., Sandbank, J., Arenzana-Seisdedos, F., Petit, I., Ben-Hur, H., Lapidot, T., and Alon, R. (1999a). The chemokine SDF-1 stimulates integrin-mediated arrest of CD34(+) cells on vascular endothelium under shear flow. J. Clin. Invest. 104, 1199–1211.

Peled, A., Petit, I., Kollet, O., Magid, M., Ponomaryov, T., Byk, T., Nagler, A., Ben-Hur, H., Many, A., Shultz, L., et al. (1999b). Dependence of human stem cell engraftment and repopulation of NOD/SCID mice on CXCR4. Science 283, 845–848.

Peranteau, W.H., Endo, M., Adibe, O.O., and Flake, A.W. (2007). Evidence for an immune barrier after in utero hematopoietic-cell transplantation. Blood 109, 1331–1333.

Peranteau, W.H., Hayashi, S., Abdulmalik, O., Chen, Q., Merchant, A., Asakura, T., and Flake, A.W. (2015). Correction of murine hemoglobinopathies by prenatal tolerance induction and postnatal nonmyeloablative allogeneic BM transplants. Blood 126, 1245–1254.

Porada, C.D., Harrison-Findik, D.D., Sanada, C., Valiente, V., Thain, D., Simmons, P.J., Almeida-Porada, G., and Zanjani, E.D. (2008). Development and characterization of a novel CD34 monoclonal antibody that identifies sheep hematopoietic stem/progenitor cells. Exp. Hematol. 36, 1739–1749.

Proytcheva, M. (2013). Bone marrow evaluation for pediatric patients. Int. J. Lab. Hematol. 35, 283–289.

Rao, S.S., Peters, S.O., Crittenden, R.B., Stewart, F.M., Ramshaw, H.S., and Quesenberry, P.J. (1997). Stem cell transplantation in the normal nonmyeloablated host: relationship between cell dose, schedule, and engraftment. Exp. Hematol. 25, 114–121.

Rechavi, E., Lev, A., Lee, Y.N., Simon, A.J., Yinon, Y., Lipitz, S., Amariglio, N., Weisz, B., Notarangelo, L.D., and Somech, R. (2015). Timely and spatially regulated maturation of B and T cell repertoire during human fetal development. Sci. Transl Med. 7, 276ra225.

Renoux, V.M., Zriwil, A., Peitzsch, C., Michaelsson, J., Friberg, D., Soneji, S., and Sitnicka, E. (2015). Identification of a human natural killer cell lineage-restricted progenitor in fetal and adult tissues. Immunity 43, 394–407.

Sacchetti, B., Funari, A., Michienzi, S., Di Cesare, S., Piersanti, S., Saggio, I., Tagliafico, E., Ferrari, S., Robey, P.G., Riminucci, M., et al. (2007). Self-renewing osteoprogenitors in bone marrow sinusoids can organize a hematopoietic microenvironment. Cell 131, 324–336.

Shcherbo, D., Merzlyak, E.M., Chepurnykh, T.V., Fradkov, A.F., Ermakova, G.V., Solovieva, E.A., Lukyanov, K.A., Bogdanova, E.A., Zaraisky, A.G., Lukyanov, S., et al. (2007). Bright far-red fluorescent protein for whole-body imaging. Nat. Methods 4, 741–746.

Skopal-Chase, J.L., Pixley, J.S., Torabi, A., Cenariu, M.C., Bhat, A., Thain, D.S., Frederick, N.M., Groza, D.M., and Zanjani, E.D. (2009). Immune ontogeny and engraftment receptivity in the sheep fetus. Fetal Diagn. Ther. 25, 102–110.

Soland, M.A., Bego, M.G., Colletti, E., Porada, C.D., Zanjani, E.D., St. Jeor, S., and Almeida-Porada, G. (2012). Modulation of human mesenchymal stem cell immunogenicity through forced expression of human cytomegalovirus US proteins. PLoS One 7, e36163.

Sugiyama, T., Kohara, H., Noda, M., and Nagasawa, T. (2006). Maintenance of the hematopoietic stem cell pool by CXCL12-CXCR4 chemokine signaling in bone marrow stromal cell niches. Immunity 25, 977–988.

Szepfalusi, Z., Pichler, J., Elsasser, S., van Duren, K., Ebner, C., Bernaschek, G., and Urbanek, R. (2000). Transplacental priming of the human immune system with environmental allergens can occur early in gestation. J. Allergy Clin. Immunol. 106, 530–536.

Takagi, S., Saito, Y., Hijikata, A., Tanaka, S., Watanabe, T., Hasegawa, T., Mochizuki, S., Kunisawa, J., Kiyono, H., Koseki, H., et al. (2012). Membrane-bound human SCF/KL promotes in vivo human hematopoietic engraftment and myeloid differentiation. Blood 119, 2768–2777.

Touraine, J.L., Raudrant, D., Royo, C., Rebaud, A., Roncarolo, M.G., Souillet, G., Philippe, N., Touraine, F., and Betuel, H. (1989). In-utero transplantation of stem cells in bare lymphocyte syndrome. Lancet 1, 1382.

Wang, L., Benedito, R., Bixel, M.G., Zeuschner, D., Stehling, M., Savendahl, L., Haigh, J.J., Snippert, H., Clevers, H., Breier, G., et al. (2013). Identification of a clonally expanding haematopoietic compartment in bone marrow. EMBO J. 32, 219–230.

Wengler, G.S., Lanfranchi, A., Frusca, T., Verardi, R., Neva, A., Brugnoni, D., Giliani, S., Fiorini, M., Mella, P., Guandalini, F., et al. (1996). In-utero transplantation of parental CD34 haematopoietic progenitor cells in a patient with X-linked severe combined immunodeficiency (SCIDXI). Lancet 348, 1484–1487.

Wiley, J.M., and Yeager, A.M. (1991). Predictive value of colony-forming unit assays for engraftment and leukemia-free survival after transplantation of chemopurged syngeneic bone marrow in rats. Exp. Hematol. 19, 179–184.

Wright, D.E., Wagers, A.J., Gulati, A.P., Johnson, F.L., and Weissman, I.L. (2001). Physiological migration of hematopoietic stem and progenitor cells. Science 294, 1933–1936.

Xu, H., Exner, B.G., Chilton, P.M., Schanie, C., and Ildstad, S.T. (2004). CD45 congenic bone marrow transplantation: evidence for T cell-mediated immunity. Stem Cells 22, 1039–1048.